Neuro-Oncology Advance Access published March 12, 2012
Neuro-Oncology
doi:10.1093/neuonc/nos002
NEURO-ONCOLOGY

The micro-RNA 199b-5p regulatory circuit involves Hes1, CD15, and epigenetic modifications in medulloblastoma

Immacolata Andolfo, Lucia Liguori, Pasqualino De Antonellis, Emilio Cusanelli, Federica Marinaro, Francesca Pistollato, Livia Garzia, Gennaro De Vita, Giuseppe Petrosino, Benedetta Accordi, Roberta Migliorati, Giuseppe Basso, Achille Iolascon, Giuseppe Cinalli, and Massimo Zollo

CEINGE, Biotecnologie Avanzate, Naples, Italy (I.A., L.L., P.D.A., E.C., F.M., L.G., G.D.V., G.P., A.I., M.Z.); Department of Biochemistry and Medical Biotechnologies (DBBM), "Federico II" University of Naples, Naples, Italy (I.A., A.I., M.Z.); Paediatric Neurosurgery, Ospedale Santobono-Pausilipon, Naples, Italy (R.M., G.C.); Haemato-Oncology Laboratory, Department of Paediatrics, University of Padova, Padua, Italy (F.P., B.A., G.B.)

Micro-RNA (miR) 199b-5p targets Hes1 in medulloblastoma, one of the downstream effectors of both the canonical Notch and noncanonical Sonic Hedgehog pathways. In medulloblastoma patients, expression of miR-199b-5p is significantly decreased in metastatic cases, thus suggesting a downregulation mechanism. We studied this mechanism, which is mediated mostly by Hes1 and epigenetic promoter modifications. The miR-199b-5p promoter region was characterized, which identified a Hes1 binding site, thus demonstrating a negative feedback loop of regulation. MiR-199b-5p was shown to be downregulated in several medulloblastoma cell lines and in tumors by epigenetic methylation of a cytosine-phosphate-guanine island upstream of the miR-199b-5p promoter. Furthermore, the cluster of differention (CD) carbohydrate antigen CD15, a marker of medulloblastoma tumor-propagating cells, is an additional direct target of miR-199b-5p. Most importantly, regulation of miR-199b-5p expression in these CD15+/CD133+ tumor-propagating cells was influenced by only Hes1 expression and not by any epigenetic mechanism of regulation. Moreover, reverse-phase protein array analysis showed both the Akt and extracellular-signal-regulated kinase pathways as being mainly negatively regulated by miR-199b-5p expression in several medulloblastoma cell lines and in primary cell cultures. We present here the finely tuned regulation of miR-199b-5p in medulloblastoma, underlining its crucial role by its additional targeting of CD15.

Keywords: CD15, epigenetic mechanism, Hes1, medulloblastoma, miR-199b-5p.

Medulloblastoma (MB) is an embryonal neuroepithelial tumor of the cerebellum. It represents the most common malignant brain tumor in childhood.[1,2] About one-third of patients with MB remain incurable despite the multimodal treatment regimens that have significantly improved survival rates for this disease. Current treatments significantly damage patient long-term survival. To improve the outcome of MB patients with high-risk disease and the quality of life of survivors, both novel therapies and new diagnostic-prognostic markers are required. Novel therapies will result from a greater understanding of the disease process, and they appear likely to involve small molecules that are designed to target specific pathways that become deregulated during oncogenesis.[3,4]

Directly implicated in MB pathogenesis is deregulation of many pathways, such as those of Wnt, Sonic Hedgehog (SHH), the erbB2 family of receptor tyrosine kinases, Akt, insulin-like growth factor 1 receptor (IGF1R), and platelet-derived growth factor receptor (PDGFR).[5] Furthermore, Notch signaling has also been linked to MB progression through promotion of a stem-cell-like state.[5,6] Several lines of evidence have linked Notch signaling to MB engraftment and progression. The Notch pathway is deregulated in MB, and

Received June 22, 2011; accepted January 6, 2012.

Corresponding Author: Massimo Zollo, CEINGE, Biotecnologie Avanzate, Via Gaetano Salvatore 486, 80145 Naples, Italy (massimo.zollo@unina.it).

there is increased expression of Hes1, which is a target of both the canonical Notch and the noncanonical SHH pathways[7–9] and is associated with poor prognosis in MB patients.[10–12] The crucial role of the Notch target gene Hes1 was emphasized by Schreck et al.,[13] who demonstrated Hes1 binding to the Gli1 first intron and its mechanism of regulation. They also demonstrated that targeting Notch and SHH simultaneously achieves more dramatic improvement than does monotherapy. Moreover, a recent phase I trial study by Fouladi et al.[14] estimated the maximum tolerated dose and characterized the pharmacokinetic properties of MK-0752, a γ-secretase (Notch/Hes1) inhibitor, in children with refractory or recurrent CNS malignancies, such as glioma, ependymoma, and MB.

Notch2 and Hes5 are overexpressed in the SHH-activated SmoA1 mouse, which suggests that activation of the SHH pathway is sufficient to induce Notch pathway genes.[8]

Previous studies using human MB cell lines have suggested that Notch signaling is required for maintenance of subpopulations of progenitor-like cells that can potentially repopulate tumors after initial therapy[15] and that inhibition of the Notch pathway can limit tumor cell growth.[11,15] Data in recent literature conversely indicate that the Notch pathway is not essential for SHH-driven MB genesis and that the maintenance of Notch signaling is not essential for the initiation, engraftment, or maintenance of SHH pathway-driven MB.[16] This interpretation is supported by the study by Julian et al.,[17] which evaluated MB formation in the absence of the recombination signal-binding protein Jκ, a convergence point for all of the Notch pathways. They showed that the canonical Notch target gene, Hes1, is not downregulated by treatment with a Notch inhibitor (MRK-003) in SmoA1 tumors. They speculated that Hes1 is both a canonical Notch target and a noncanonical SHH target gene, whereas Notch1, Notch2, and Hes5 are targets of Notch signaling but not of SHH signaling. In the setting of chronic SHH pathway activation in the SmoA1 cerebellum, γ-secretase inhibitor treatment alters Notch1, Notch2, and Hes5 expression but does not affect SHH-mediated Hes1 expression.[14]

Supporting data from the literature demonstrate that micro-RNAs (miRNAs), small noncoding RNAs, have crucial roles in MB progression through their targeting of important proteins/pathways that are already known to be involved.[18–24] In our previous study,[25] we identified miRNA (miR)-199b-5p as a regulator of the Notch pathway through its targeting of Hes1. We demonstrated that miR-199b-5p overexpression impairs both the proliferation rate and the anchorage-independent growth of MB cells in vitro, and impairs the engrafting potential of MB cells in the cerebellum of athymic/nude mice, decreasing the MB stem-cell-like (cluster of differentiation [CD] 133+) subpopulation of cells. Furthermore, in MB patients, the expression of miR-199b-5p in nonmetastatic cases was significantly higher than in metastatic cases, which suggests a downregulation mechanism through epigenetic or genetic alterations. Upon induction of the demethylation processes using 5-aza-2′-deoxycytidine (AZA), increased miR-199b-5p expression was seen in a panel of MB cell lines, which further supports an epigenetic mechanism of regulation.[25]

Studies of epigenetic changes in MB development offer significant potential for improved understanding of its molecular pathogenesis.[26,27] Many studies have suggested that multiple loci undergo changes in methylation status during MB development, although relatively few gene-specific events have been identified to date.[26–28] Moreover, it is known that most methylation alterations in cancers occur not only in promoters but also in sequences at up to a 2-kb distance, which are termed "cytosine—phosphate—guanine (CpG) island shores."[29] CpG island shore methylation is strongly related to gene expression.[29] Epigenetic mechanisms are also responsible for aberrant miRNA expression in several malignancies.[30–34] Thus, it is believed that the primary role of miRNAs is to modulate the dynamics of regulatory networks.[35]

Here, we investigated the regulation of miR-199b-5p expression during MB progression. We have identified a feedback regulation loop by its target gene *Hes1*, the promoter region of which we have characterized, and we have studied the methylation of a CpG island upstream of its promoter. In search of other possible direct targets of miR-199b-5p, we identified CD15, a known marker of cancer stem cells in MB, and we studied CD15 regulation in CD15+/CD133+ cells. Overexpression of miR-199b-5p also impairs the Akt and extracellular signal-regulated kinase (ERK) signaling pathways, both of which are crucial protein networks involved in the maintenance of cancer stem cells. This allowed us to further characterize other signaling pathways that are affected by miR-199b-5p regulation, providing findings that are of relevance for future therapeutic applications.

Material and Methods

Cell Culture

Daoy, UW228, HEK-293, ONS 76, D341, and D245 human MB cell lines and HEK-293 were obtained from the American Type Culture Collection. The Daoy and UW228 cells were maintained in Eagle's minimum essential medium (Sigma) supplemented with 10% fetal bovine serum (FBS), 10 U/mL penicillin, and 0.1 mg/mL streptomycin (Celbio Pero). The D341 and D245 cells were maintained in Eagle's minimum essential medium (Sigma) supplemented with 20% FBS, 10 U/mL penicillin, and 0.1 mg/mL streptomycin (Celbio Pero). HEK-293 cells were maintained in Dulbecco's modified Eagle's medium (DMEM; Sigma) supplemented with 10% FBS, 10 U/mL penicillin, and 0.1 mg/mL streptomycin. The ONS 76 cells were maintained in Roswell Park Memorial Institute medium (Sigma) supplemented with 10% FBS, 10 U/mL penicillin, and 0.1 mg/mL streptomycin.

Primary Human Medulloblastoma Cultures and Patient Samples

Primary cultures of human MB were derived from a tumor of a 6-month-old female (P.MB1; desmoplastic histotype) and a 4-year-old male (P.MB2; classic histotype). These patients underwent surgery at the Neurochirurgia Pediatrica, Ospedale Santobono-Pausilipon, Naples, Italy, under written consent. Briefly, samples of these tumors were first obtained to allow full neuropathological evaluation and diagnosis, as required for the clinical management of the disease. The site of origin of the tumor samples was the cerebellum. Sterile dissections from the tumor biopsies were dissociated and plated in 6-well tissue-culture plates and expanded in DMEM supplemented with 20% FBS, 20 ng/mL recombinant human epidermal growth factor (EGF), and 10 ng/mL recombinant human b-fibroblast growth factor (Becton Dickinson). These P.MB1 and P.MB2 cells were subsequently maintained in DMEM (with L-glutamine), supplemented with 10% FBS, and were used at low passage numbers (below passage 20 for all of these studies). A total of 15 surgical MB specimens were used for the methylation analyses. Informed consent was obtained before the analysis of the tumor samples. All of the specimens were obtained at the time of diagnosis, prior to radiation therapy or chemotherapy, and 29 were subjected to histopathological review according to the WHO criteria. Control human tissues were obtained from the National Institute of Child Health and Human Development Brain and Tissue Bank for Developmental Disorders at the University of Maryland.

Vector Cloning

Pre-miR-199b-5p was cloned into a pcDNA3.1 vector (Promega) using the EcoRI–XhoI restriction sites, as described by Garzia et al.[25] The CD15 full-length 3′ untranslated regions (UTRs) were divided into 2 fragments of 2340 bp and 1832 bp and were cloned into the pRL-TK renilla vector (Promega), downstream of the coding region of renilla luciferase, in the XbaI site. The 3′-UTR of CD15 was amplified from genomic DNA. The primer sequences are available upon request.

The promoter regions of miR-199b-5p were divided into 3 phosphogluconolactonase (PGL) fragments: PGL3-R2, PGL3-R3, and PGL3-R1(R2 + R3), which were cloned upstream of the luciferase gene into a PGL3 vector in the Hind III and Xho I sites after the amplification from the genomic DNA. The mutant constructs were cloned upstream of the luciferase gene into a PGL3 vector in the Hind III and Xho I sites, as PGL3 del 0, PGL3 del 1, PGL3 del 2, PGL3 del 3, PGL3 del 4, and PGL3 del 5. The mutant constructs were amplified from genomic DNA in overlapping fragments.

Target Validation of CD15 by Luciferase Assays

To evaluate the activity of miR-199b-5p for repression of full-length luciferase 3′-UTR constructs, the pcDNA3.1 miR-199b-5p construct (0.5 μg) and the pRL-TK 3′-UTR target construct (0.1 μg) were cotransfected into Daoy and HEK-293 cells, using the TransIT-Low Toxicity (LT) 1 transfecting reagent (Mirus, Bio Corporation), with a PGL3 cytomegalovirus (CMV) firefly luciferase vector for normalization. Luciferase activities were analyzed using a Dual Luciferase Reporter assay system (Promega).

RNA Isolation, cDNA Preparation, and Quantitative Real-time PCR Analysis

Total RNA was extracted from the cell lines using Trizol reagent (Invitrogen). Synthesis of cDNA from total RNA (2 μg) used Super Script II First Strand kits (Invitrogen). Quantitative real-time PCR (qRT-PCR) was performed using the SYBR-green method, following standard protocols with an Applied Biosystems ABI PRISM 7900HT Sequence Detection system. Relative gene expression was calculated using the $2^{(-\Delta Ct)}$ method, where ΔCt indicates the differences in the mean cycle threshold (Ct) between selected genes and the internal control.[36] QRT-PCR primers for each gene were designed using Primer Express software, version 2.0 (Applied Biosystems). Primer sequences are available upon request. The significance of the gene expression differences were determined using Student's *t*-tests; statistical significance was established at $P < .05$. All statistical analyses were performed using Excel, as included in the Microsoft Office 2007 suite.

Western Blotting

Total lysates of 50 μg were loaded and run on 12% polyacrylamide gels, which were then blotted onto polyvinylidene difluoride membranes (BioRad). These membranes were incubated with the following antibodies: polyclonal rabbit anti-Hes1 (1:500; ABCAM), polyclonal anti-CD133 (1:500; ABCAM) and anti-CD15 (1:500; BD Bioscience), and monoclonal anti-CD15 (1:100; BD Bioscience). An anti–β-actin antibody (1:5000; Sigma) was used in the control for the equal loading of the total lysates.

TaqMan miRNA Assay

Reverse transcriptase reactions.—Reverse transcriptase reactions for miR-199b-5p and mMU6 were performed with 40 ng RNA samples, 50 nM stem-loop reverse transcriptase primer, 1x reverse transcriptase buffer (P/N 4319981, Applied Biosystems), 0.25 mM of each deoxyribonucleotide triphosphate, 3.33 U/mL MultiScribe reverse transcriptase (P/N 4319983, Applied Biosystems), and 0.25 U/mL RNase inhibitor (P/N N8080119; Applied Biosystems). These 15-μL reactions were incubated in an Applied Biosystems 9700

Thermocycler for 30 min at 16°C, 30 min at 42°C, and 5 min at 85°C, and then held at 4°C.

Quantitative PCR.—QRT-PCR was performed using a standard TaqMan PCR kit protocol on an Applied Biosystems 7900HT Sequence Detection system. The 20-μL PCRs included 2 μL reverse transcriptase product, 10 μL TaqMan Universal PCR Master Mix (Applied Biosystems), and 0.2 mM TaqMan probe (for miR-199b-5p and mMU6). The reactions were incubated in a 96-well plate at 95°C for 10 min, followed by 60 cycles of 95°C for 15 s, and 60°C for 1 min.

Chromatin Immunoprecipitation Assay

Chromatin immunoprecipitation (ChIP) studies were performed essentially as described in the Upstate ChIP assay kit. Pre-cleared cell lysates were incubated overnight at 4°C with 5 μg anti-Hes1 antibody (Santa Cruz Biotechnology). To detect specific DNA segments, 10 μL DNA were used for the PCRs, with the following primers: Hes1 sense -CTTCTGCCTCCTTTGACGTG- and antisense -GGGAGGAGAGGAGGAAGTTG- repressor element-1 silencing transcription factor sense -AGAGCAGGCAGGGAGATTTT- and antisense -GACCATCCTTACCCATGTCG-, and cyclin D2 sense -CCTGGAGTGAAATACACCAAAGGGC- and antisense -CCTCACTCTGCCAGGCTTTCTCC-.

Promoter Assay

Daoy and HEK-293 cells were plated in 6-well plates and transfected using TransIT-LT1 transfecting reagent (Mirus, Bio Corporation), with the PGL3-R2 (2 μg), PGL3-R3 (2 μg), and PGL3-R1(2 μg) vectors. The next morning, one 6-well plate was treated with N-[N-(3,5-difluorophenacetyl)-1-alany1]-S-phenyglycine *t*-butyl ester (DAPT) for 12 h and Sh-Hes1 for 72 h. The pRL-CMV vector (100 ng) was used for normalization. The same promoter assay was carried out with UW228 cells transfected using FuGENE 6 transfecting reagent (Promega). Luciferase activities were analyzed as above, using a Dual Luciferase Reporter assay system (Promega).

CD133/CD15 Flow Cytometry Analyses and Cell Sorting

MB cells ($3–5 \times 10^6$ cells/mL) were incubated with a human anti-CD15 antibody (fluorescein isothiocyanate conjugated, 1:20; Immunotech) and a human anti-CD133 antibody (clone AC133/2-PE, 1:20; Miltenyi Biotec), as previously described.[37] The cells were analyzed on a MoFlo High Performance Cell Sorter (Beckman Coulter) and then sorted on the basis of CD15 and CD133 expression. The CD15 versus CD133 dot plot revealed the populations of interest that were sorted: the CD15+/CD133+ and CD15−/CD133− cell fractions, which were selected by setting the appropriate sorting gates. The relative percentages of the 2 different subpopulations were calculated based on the live gated cells (as indicated by physical parameters, side scatter, and forward scatter). Unlabeled cells were first acquired to ensure the labeling specificity. Cells to be sorted were resuspended in buffer (bovine serum albumin 0.5%, EDTA 2 mM in phosphate buffered saline [PBS]) and kept cold until sorted. The sorted cells were collected in tubes containing growth medium. After sorting, an aliquot of sorted cells was run on a MoFlo cell sorter to determine the purity of the 2 populations.

Methylation Assay

The methylation status of the CpG island located upstream of miR-199b-5p (359 bp) was assessed by bisulfite modification of genomic DNA (500 ng) extracted from the 4 MB cell lines (DAOY, UW228, D425, and D341), the 15 MB tumor samples, the 5 relative DNAs extracted from peripheral blood of the same patients, and the 3 samples from normal cerebellum, using the MethylCode Bisulfite Conversion kits (Invitrogen). To determine the methylation status of the CpG island in each sample, the amplified bisulfite-sequencing PCR products were cloned into the pCR2.1-TOPO vector (Invitrogen), and 10 to 12 clones from each sample were sequenced using an ABI3130x automated sequencer (Applied Biosystems), as described by Toyota et al.[38]

Reverse-phase Protein Arrays

The MB cells were lysed in an appropriate lysis buffer (Tissue Protein Extraction Reagent; Pierce) containing protein inhibitors (300 mM NaCl, Sigma; 1 mM orthovanadate, Sigma; 200 mM Pefabloc [4-(2-aminoethyl) benzenesulfonyl fluoride hydrochloride], Roche; 1 μg/mL aprotinin, Sigma; 5 mg/mL pepstatin A, Sigma; and 1 mg/mL leupeptin, Sigma). They were then diluted to 1 mg/mL in 2× Tris-glycine sodium dodecyl sulfate sample buffer (Invitrogen Life Technologies) plus 5% β-mercaptoethanol. Reverse-phase protein arrays (RPPAs) were printed in duplicate, with whole-cell protein lysates, as described by Petricoin et al.[39,40] Briefly, the lysates were printed on glass-backed nitrocellulose array slides (FAST slides, Whatman) using an Aushon 2470 arrayer (Aushon Biosystems). Each lysate was printed in a dilution curve that provided undiluted lysate, 1:2, 1:4, 1:8, and negative control dilutions. A431, HeLa pervanadate (BD Biosciences), and Jurkat apoptotic (Cell Signaling Technology) cell lysates were printed on each array, for quality control assessments. The protein microarray slides were prepared for immunostaining by washing with PBS without calcium or magnesium and blocking with I-Block in PBS plus 0.5% Tween-20 (Applied Biosystems) for a minimum of 1 h. Protein expression on the arrays was assessed through a catalyzed signal-reporter system. Briefly, the slides were placed on an automated slide stainer (Autostainer; Dako) and immunostained according to the manufacturer's instructions (CSA kit; Dako).[41,42]

A set of specific, validated antibodies to phosphorylated or cleaved proteins in the different pathways was used to immunostain the RPPAs for CDK2 and Annexin II (Biosource International), Akt S473, MEK 1-2 S217-221, ERK 1-2 (T202-204), P90K S3780, AKT, PKC S657, and AMPKa (Cell Signaling Technology). The negative control slide was incubated with the antibody diluent without the primary antibody. The secondary antibody probe was goat anti-rabbit immunoglobulin G, heavy and light chain (1:5000 dilution; Vector Laboratories). The total protein per microarray spot was determined with Fast Green forchlorfenuron protein blot stain (Sigma), according to the manufacturer's instructions, to estimate the total protein of each printed sample, to ensure that the intensity values were not dependent on changes in the concentrations of the printed lysates. Each array was scanned, the spot intensities analyzed, and the data normalized to total protein/spot, with a standardized, single data value generated for each sample on the array using the Microvigene Software (VigeneTech), which was specifically developed for RPPA analysis.

Cell Proliferation Assay

Proliferation of UW228 and ONS 76 cells was assessed by seeding the cells infected with adenovirus carrying miR-199b-5p (AdV 199b-5p) and its control (AdV Mock) in medium containing 10% FBS in 96-well plates (3000 cells/well). Cell viability was analyzed after 72 h using the MTS [3-(4,5-dimethylthiazol-2-yl)-5-(3-carboxymethoxyphenyl)-2-(4-sulfophenyl)-2-H-tetrazolium] assay with the Cell Titer 96 Aqueous One Solution Cell Proliferation Assay (Promega), and cell survival curves were established.

Colony Formation in Soft Agar

ONS 76 cells infected with adenovirus carrying miR-199b-5p (AdV 199b-5p) and its control (AdV Mock) were plated at 2×10^5 cells/well in triplicates in 0.5% agarose-coated 6-well plates in the presence of medium containing 10% fetal calf serum without or with inhibitors. After 2 weeks, the colonies were stained with crystal violet, and the numbers of colonies were counted.

Monolayer Wound-healing Assay

Daoy, UW228, and ONS 76 MB cells were infected with adenovirus carrying miR-199b-5p (AdV 199b-5p) and its control (AdV Mock) for 48 h. The cells were then plated in wells of a 6-well culture dish. Two (or more) parallel scratch wounds of approximately 400 μm width were made perpendicular to the marker lines with a blue P1000 pipette tip (Corning). The wounds were observed after 24 h using phase contrast microscopy.

Migration Assays

Migration of MB cells through membranes with 8 Am pores was assessed using Transwell filter inserts assembled in 24-well plates (Corning). Daoy, UW228, and ONS 76 cells were infected with adenovirus carrying miR-199b-5p (AdV 199b-5p) and its control (AdV Mock) for 72 h. Cells (5×10^4 in 200 μL serum-free medium) were then placed into the upper well of the membrane. Medium (500 μL) containing 0.5% FBS for Daoy and ONS 76 cells and 10% FBS for UW228 cells was added to the lower chamber as the chemoattractant. The assay plates were incubated at 37°C and 5% CO_2 for 4 h for Daoy and ONS76 cells and for 12 h for UW228 cells. Quantification of migration through the porous membranes was carried out by counting the stained cells (0.1% crystal violet/20% methanol) using a microgrid.

Statistical Analysis

All of the data are presented as means ± standard errors. Statistical significance was calculated using the Mann-Whitney test and Student's *t* test. The correlation analysis was calculated using Spearman's rank correlation coefficient and Pearson's correlation coefficient. $P < .05$ was considered as statistically significant.

Results

Hes1 Inhibition Increases miR-199b-5p Expression

Previously, we identified miR-199b-5p function by targeting the regulation of Hes1, and we further demonstrated miR-199b-5p downregulation during MB development and metastasis processes.[25] We also wanted to understand the mechanisms by which miR-199b-5p is negatively regulated during MB progression.

To verify the involvement of Hes1 in miR-199b-5p regulation, we analyzed the expression of miR-199b-5p after treatment with DAPT (a γ-secretase complex inhibitor) and by Hes1 silencing (small interfering [si]RNA technology). The Daoy MB cell line was treated with DAPT for 6 h and 12 h. We confirmed the downregulation of Hes1 by Western blotting (Supplementary material, Fig. S1A, left). Then, we analyzed miR-199b-5p expression within these assays using miRNA TaqMan assay, which demonstrated that after DAPT treatment and Hes1 downregulation, miR-199b-5p expression increased gradually, with significant upregulation 12 h after treatment (Supplementary material, Fig. S1A, right). These data provided the first evidence of regulation of miR-199b-5p by Hes1. Furthermore, direct evidence of inhibition was carried out by inhibition of Hes1 expression through the use of siRNA technology. These data confirmed the downregulation of Hes1 by Western blotting (Supplementary material, Fig. S1B). We then analyzed miR-199b-5p expression, demonstrating that

miR-199b-5p expression also significantly increased after the silencing of Hes1. Altogether, these data demonstrated that miR-199b-5p expression is negatively controlled by the repressive transcriptional function of Hes1.

We then speculated that Hes1 can bind directly to the miR-199b-5p promoter region to downregulate its expression. For this reason, we looked at the genomic region: miR-199b-5p is transcribed in an antisense orientation in an intronic region of the dynamin 1 (*Dnm1*) gene[43] on chromosome 9 (9q34.11). We first excluded the possible mechanism of miR-199b-5p processing by the *Dnm1* gene. We found that after DAPT treatment and Hes1 inhibition (which increased miR-199b-5p expression), Dnm1 expression did not change (data not shown). For this reason, we examined the region upstream of miR-199b-5p to characterize its promoter. The conservation of the genomic region upstream of miR-199b-5p between human and mouse was analyzed using mVISTA (http://genome.lbl.gov/vista/mvista/submit.shtml). This analysis showed that the regions indicated as R2 and R3 were the most conserved regions (Supplementary material, Fig. S1C, top). The regions R2, R3, and R1 (R2 + R3) were then cloned into the reporter plasmid, the PGL3-promoter vector, which contained a minimal SV40 promoter upstream of firefly luciferase cDNA, as illustrated in the schematic model in the Supplementary material, Fig. S1C (bottom). These constructs were used for further promoter analyses.

Hes1 Binds to the miR-199b-5p Promoter Region and Controls its Expression by a Negative Feedback Loop of Regulation

The vectors PGL3 R2, PGL3 R3, and PGL3 R1 (described in the Supplementary material, Fig. S1C) were then transfected into the Daoy cell line, some treated with DAPT. The R2 region showed greater luciferase activity compared with the R3 and R1 regions (Fig. 1A, left). Furthermore, treatment with DAPT, and the consequent Hes1 downregulation, increased the luciferase activity of the R2 region. We then performed a bioinformatics search for possible transcription factor binding sites for Hes1 (MatInspector software; www.genomatix.de) in the human genomic sequence of R2, upstream of the miR-199b-5p transcriptional unit. There is one Hes1 site in the R2 region, which we mutated in the PGL3 R2 vector by site-direct mutagenesis. The results show that the mutated R2 region has increased luciferase activity with respect to the wild-type R2 region, thus demonstrating that inhibition of Hes1 increases the luciferase activity of the R2 region (Fig. 1A, right panel). Similar results were obtained by inhibition of Hes1 using one siRNA vector specifically inhibiting Hes1 expression also in HEK-293 cells (data not shown) and in UW228 cells (classic MB histotype cells), which demonstrated similar results (Supplementary material, Fig. S2A).

We then analyzed the minimal promoter region of miR-199b-5p using a mutational cloning strategy. We subcloned the R2 region as 6 overlapping fragments of about 200 bp. We then cloned these fragments into the PGL3 vector upstream of the firefly luciferase gene, as illustrated in the schematic model of the constructs in Fig. 1B (left). Luciferase assays with these deletion mutant constructs were performed in the Daoy and UW228 cell lines (Fig. 1B and Supplementary material, Fig. S2B). We observed that regulation of the region PGL3 del 1 was cell dependent, mainly because in the Daoy cell line there was higher luciferase in comparison with the PGL3 del 0 construct, while the PGL3 del 1 construct showed similar luciferase activity in comparison with the PGL3 del 0 construct in UW228 cells. The smallest fragment (200 bp, PGL3 del 5) upstream of miR-199b-5p still activated luciferase transcription. As expected by MatInspector analysis, this region was predicted to contain the core promoter element (core promoter motif 10 elements). Furthermore, we demonstrated the direct binding of Hes1 to the R2 region by ChIP assays in UW228, ONS 76, and Daoy MB cells (Fig. 1C). Isolated chromatin from the MB cells was immunoprecipitated using control immunoglobulin G or an anti-Hes1 antibody, followed by PCR analysis with primers targeted to R2 sequences, according to the protocol shown by Abderrahmani et al.,[44] which uses *Rest* as a positive control and *Cyclin D2* as a negative control.

Overall, these data demonstrate that miR-199b-5p has an autonomous promoter region to which Hes1 binds that, in turn, regulates the expression of miR-199b-5p through a negative feedback loop.

Epigenetic Regulation of miR-199b-5p Expression

In our previous studies, treatment of MB cell lines with AZA, a chemical analog of cytidine and a methyltransferase inhibitor that promotes demethylation, resulted in upregulation of miR-199b-5p expression in Daoy, MED8a, and UW228 MB cells.[25] Here, we analyzed the epigenetic regulation of miR-199b-5p starting with the upstream region and using the EMBOSS CpGPlot (EMBL-EBI) tool to search for CpG islands. We found a CpG island 3 kb upstream of the 5′-site of miR-199b-5p. This island could thus contain an enhancer of the promoter, or it could be a part of the pre-miR-199b-5p region. We first analyzed miR-199b-5p expression in the Daoy, UW228, D425, and D341 MB cell lines (Fig. 2A). Then, we studied the methylation status of this region using bisulfite sequence methodology in several MB cell lines, 15 MB tissue samples (using DNA from the peripheral blood of the same patients as the internal controls), and 3 healthy human cerebellum tissue samples (Fig. 2B and C). We analyzed the percentages of methylated CpG islands (see Methods section) in the Daoy, UW228, D425, and D341 MB cell lines untreated and treated with AZA (Fig. 2B). We found that these percentages of methylated CpG islands significantly decreased,

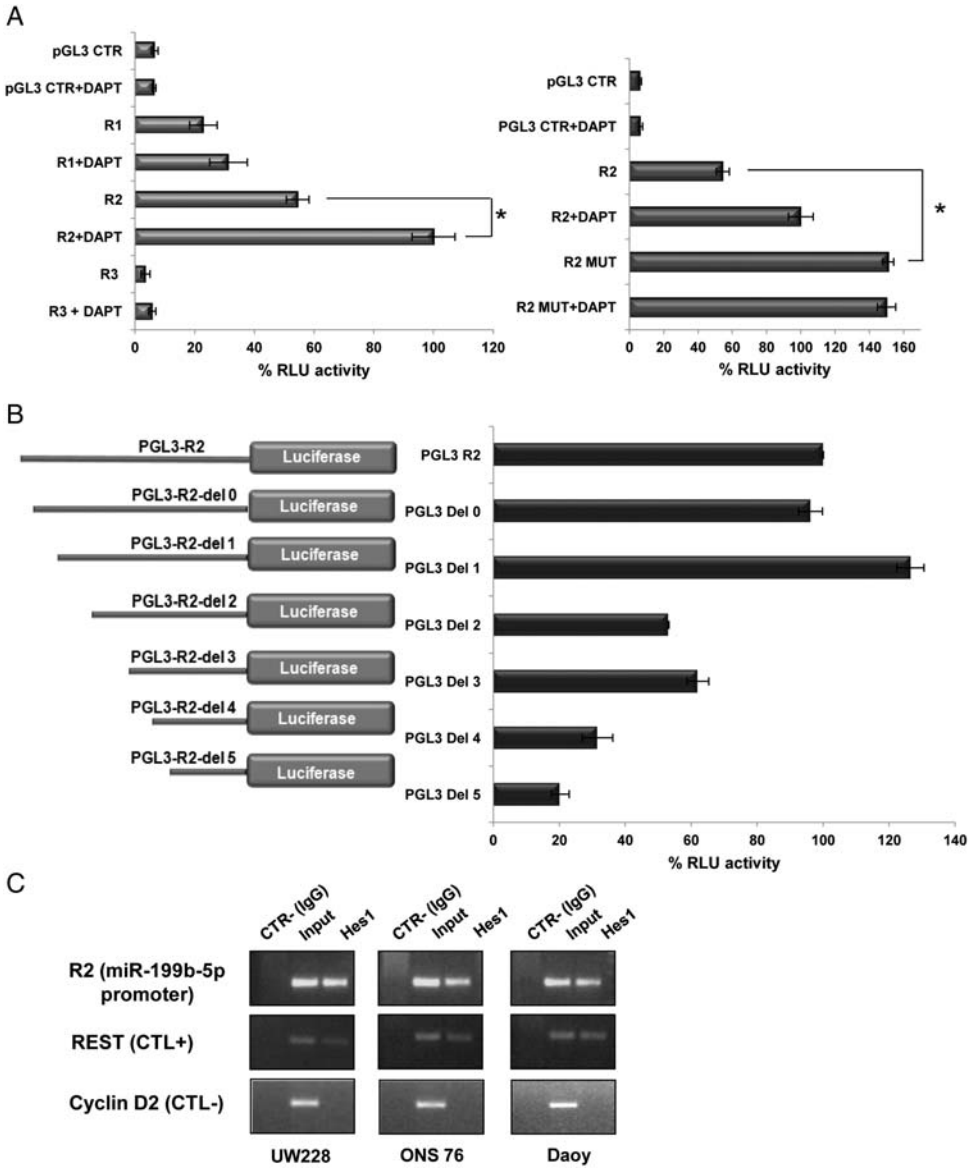

Fig. 1. MiR-199b-5p promoter characterization. (A) Luciferase assays in the Daoy cell line, showing percentage luciferase activities of the R1, R2, and R3 (R1 + R2) regions (upstream regions of miR-199b-5p) without and with DAPT treatment (left), and of the R2 region mutated in the Hes1 binding site (R2 MUT; right). Data are means ± standard errors of 3 independent experiments. *$P = .02$ (left), 0.03 (right). (B) Left: Schematic representation of the constructs for the luciferase assay, with the regions upstream of miR-199b-5p divided into fragments of about 200 bp, cloned into the PGL3 vector upstream of the firefly luciferase gene. Right: Luciferase assays in the Daoy cell line, showing the percentage of luciferase activities of the regions in the left panel. Data are means ± standard errors of 3 independent experiments. (C) Representative chromatin immunoprecipitation assays of the R2 region with a polyclonal anti-Hes1 antibody, showing Hes1 binding to R2 in UW228, ONS 76, and Daoy cells. *Rest* and Cyclin D2 are the positive and negative controls, respectively.

which demonstrated direct correlation between overexpression of miR-199b-5p after AZA treatment and demethylation of the region upstream of its promoter region. The percentage of methylated CpG islands was higher in samples from MB patients than in healthy cerebellum ($P = .02$), and this was also observed in the DNA from MB tissues compared with the corresponding DNA extracted from the peripheral blood of the same patients, thus normalizing interindividual variations and further demonstrating the specificity of the methylation pattern on the regulation of miR-199b-5p expression (Fig. 2C). We then analyzed the correlation between miR-199b-5p expression and the percentage of CpG island methylation in MB tissues, using Spearman's rank correlation test, which demonstrated an inverse correlation (Spearman's rho $= -0.5$; $P = .03$) (Fig. 2D).

Finally, we analyzed the expression of miR-199b-5p after the combination of DAPT (Hes1 inhibition) and AZA (demethylation) treatment. Overall, we observed that the combined treatment (DAPT and AZA) increased miR-199b-5p expression more than did the single treatment (Fig. 2E and F). At this stage, we can

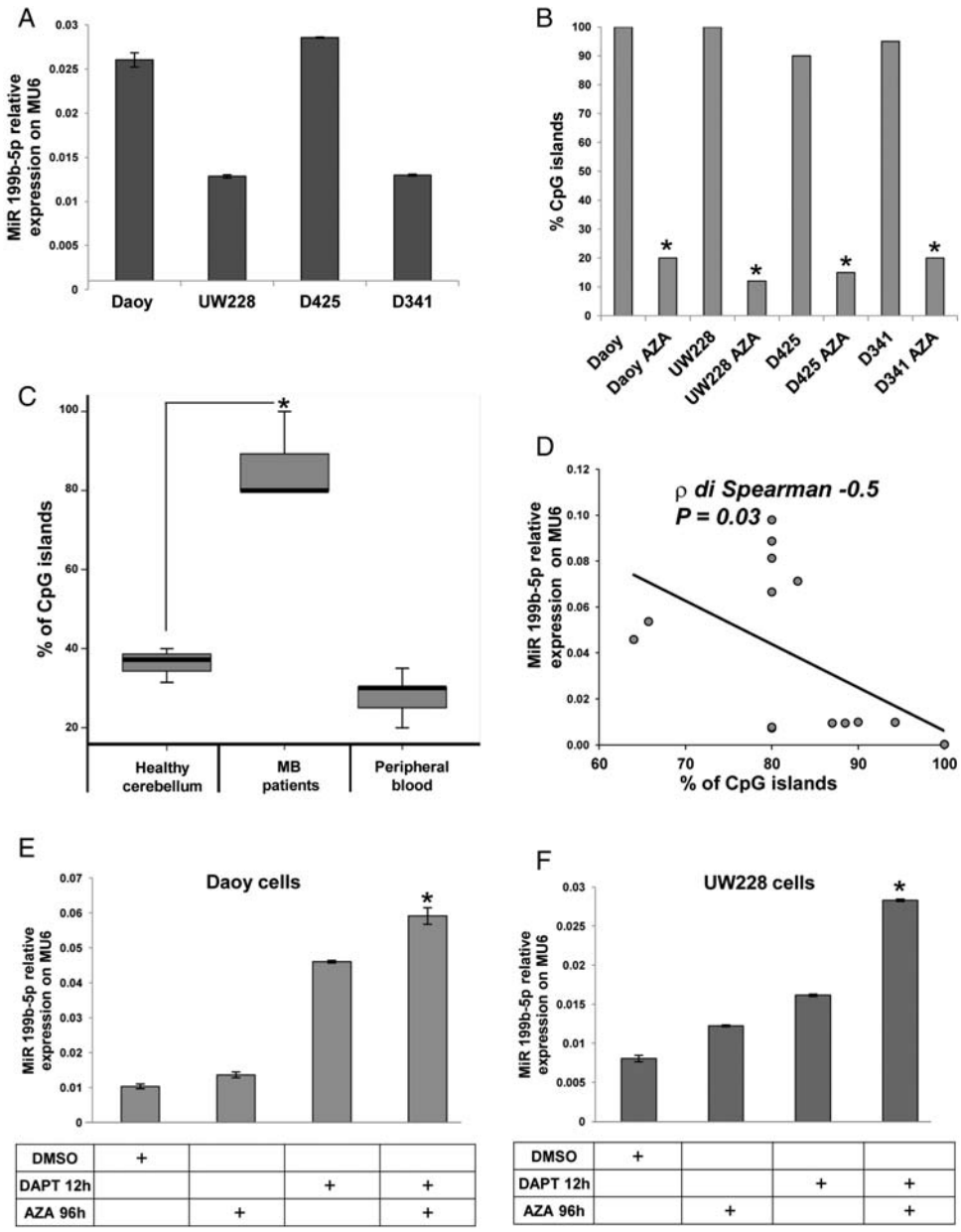

Fig. 2. Epigenetic control of miR-199b-5p in human MB cells and in tissues from MB patients. (A) Relative expression levels of miR-199b-5p on MU6 by miRNA TaqMan assay in Daoy, UW228, D425, and D341 MB cells. (B) Percentages of methylated CpG islands in the upstream region of miR-199b-5p in MB cell lines (Daoy, UW228, D425, and D341) without and with AZA treatment (as indicated). Data are means ± standard errors of 3 independent experiments. *$P < .001$, vs. without AZA, respectively. (C) Box plot showing the percentages of methylated CpG islands in the upstream region of miR-199b-5p, across 15 MB tissues, 5 peripheral blood (DNA extracted from peripheral blood of the corresponding patients), and 3 healthy cerebellum samples. Data are means ± standard errors of 3 independent experiments. *$P = .02$ for MB (15) vs. healthy cerebellum (3). (D) Correlation analysis by Spearman rank test showing an inverse correlation between percentages of CpG islands upstream of the miR-199b-5p promoter (*x* axis) and miR-199b-5p expression (*y* axis) in 15 MB tissues (ρ of Spearman −0.5; *$P = .03$). (E and F) Relative expression of miR-199b-5p on mMU6 by miRNA TaqMan assay in Daoy and UW228 cells treated with AZA (96 h), DAPT (12 h), and the combination of DAPT plus AZA (96 h). *$P = .03$ (left) and *$P = .02$ (right). Data are means ± standard errors of 3 independent experiments.

conclude that miR-199b-5p expression is regulated by 2 independent mechanisms of action, an Hes1 negative feedback loop and Hes1 promoter methylation, which cooperate to downregulate miR-199b-5p expression in MB.

MiR-199b-5p Directly Targets CD15 in Medulloblastoma

In light of the discovery of CD15 as a new marker of tumor-propagating cells in MB,[45,46] and because of the

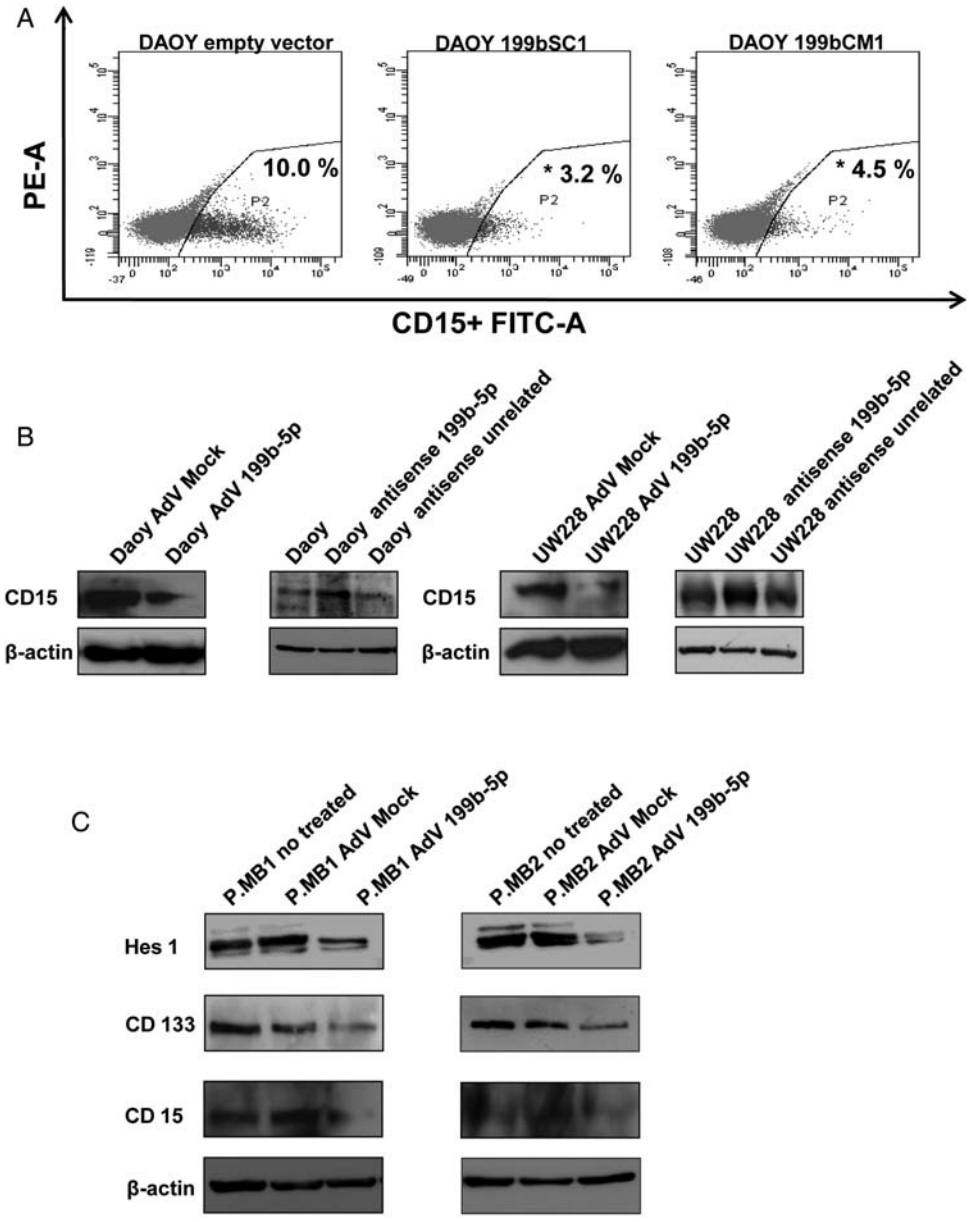

Fig. 3. Downregulation of CD15+ cells in MB cell lines and in primary human MB cultures after overexpression of miR-199b-5p. (A) Representative fluorescence-activated cell sorting analysis showing CD15+ cells in the empty vector clone and in the Daoy stable clones overexpressing miR-199b-5p (199bSC1 and 199bCM1; as indicated). *$P = .04$ (middle), 0.03 (right). (B) Representative Western blotting showing CD15 protein expression using a monoclonal anti-CD15 antibody, in Daoy and UW228 cells infected with adenovirus carrying miR-199b-5p, and in Daoy and UW228 cells treated with an inhibitor of miR-199b-5p (as indicated). β-Actin expression shown for normalization. (C) Representative Western blotting showing Hes1, CD133, and CD15 protein expression in P.MB1 and P.MB2 human MB primary cultures infected with adenovirus carrying miR-199b-5p, and the relative controls (mock) (as indicated). β-Actin expression shown for normalization. Data are all representative of 3 independent experiments.

downregulation of CD133+ cells (a well-known marker of tumor-propagating cells in MB) in the Daoy stable clones overexpressing miR-199b-5p, we asked whether or not miR-199b-5p overexpression could influence expression of CD15. We approached this question using our previous miR-199b-5p overexpressing MB clones.[25] Here, in the 199bSC1 and 199bCM1 Daoy stable clones, the percentage of CD15+ cells significantly decreased in comparison with the Daoy empty vector clone, as seen by fluorescence-activated cell-sorting analysis (3.2% and 4.5%, respectively, vs. 10.0%; Fig. 3A). Thus, with the hypothesis that *CD15* is another direct target of miR-199b-5p, we used an *in silico* analysis approach using the Probability of Interaction by Target Accessibility miRNA-target-prediction database[47] to determine whether the 3′-UTR of CD15 contains sites that can be recognized by miR-199b-5p. We found 5 predicted sites for miR-199b-5p in the 3′-UTR of the

CD15 mRNA. To confirm these *in silico* predictions, a renilla luciferase reporter assay was constructed that contained the 3′-UTR of human *CD15* mRNA, the expression of which was driven by the thymidine kinase (Tk) promoter (Tk-ren/CD15) (Supplementary material, Fig. S3A). We cloned the 3′-UTR of *CD15* mRNA with its division into 2 fragments of 2340 bp (containing 2 sites with ΔΔGs of −14.4 and −8.4) and 1832 bp (containing 3 sites with ΔΔGs of −17.8, −7.8, and 8.9), downstream of the renilla luciferase coding region in the Tk-renilla vector. Pre-miR-199b-5p was cloned into a mammalian expressing vector (pcDNA3.1). The reporter construct (Tk-ren/CD15) and miR-199b-5p were cotransfected into Daoy cells, with the PGL3-CMV firefly luciferase vector to normalize for transfection efficiency. Interestingly, the relative luciferase activity was markedly decreased in cells cotransfected with the Tk-ren/CD15-1 construct and miR-199b-5p (by 40%) ($P = .005$) (Supplementary material, Fig. S3A, left). This indicated that miR-199b-5p binds to the 3′-UTR of CD15-1, resulting in decreased luciferase protein expression. As a further control, miR-199b-5p mutated in its seed region sequence was cotransfected with Tk-ren/CD15, with the consequent return of the luciferase activity (Supplementary material, Fig. S3A, left). The second fragment, Tk-ren/CD15-2, did not show any significant reduction in luciferase activity when cotransfected with miR-199b-5p (Supplementary material, Fig. S3A, right). Similar data were obtained in HEK-293 cells (data not shown). Then, as a further control, we carried out the same luciferase assays with inhibition of the endogenous levels of miR-199b-5p using a miRNA antisense inhibitor. As shown in the Supplementary material, Fig. S3B, inhibition of miR-199b-5p endogenous levels increased the luciferase activity of the Tk-ren/CD15 1 reporter construct but not of the Tk-ren/CD15 2 reporter construct. We thus concluded at this stage that miR-199b-5p binds the 3′-UTR of *CD15* mRNA, thus impairing its expression.

We further confirmed the inhibition of CD15 expression by miR-199b-5p through infection of Daoy (desmoplastic MB histotype) and UW228 (classic MB histotype) MB cells for 72 h with an adenovirus carrying miR-199b-5p, as shown by the Western blotting analysis in Fig. 3B. Moreover, as for a luciferase assay, we inhibited the endogenous levels of miR-199b-5p using a miRNA antisense inhibitor, which after transfection specifically inhibited endogenous miRNA expression in Daoy and UW228 cells. After 48 h of transfection, there was increased endogenous expression of the target CD15 at the protein level, as shown in Fig. 3B. This provided additional evidence that miR-199b-5p targets CD15 in MB.

MiR-199b-5p Impairs Tumor-propagating Cells in Primary Cultures of Human Medulloblastoma

We further extended our studies to primary MB cells that were freshly isolated from surgical specimens from children with MB. Adherent P.MB1 (desmoplastic MB) and P.MB2 (classic MB) cells were infected with an adenovirus carrying miR-199b-5p, in the same manner as for the Daoy and UW228 cells. We used adenovirus green fluorescent protein expression AdV Mock and AdV 199b-5p as the controls for infection efficacy, as shown in the Supplementary material, Fig. S3C. In these primary cultures of human MB, we confirmed inhibition of Hes1 protein expression and impairment of the tumor-propagating cell markers CD15 and CD133 by Western blotting in primary MB cells (Fig. 3C). Similar levels of inhibition were observed in ONS 76 (classic histotype) MB cells (see Supplementary material, Fig. S4A).

MiR-199b-5p Regulation in Medulloblastoma Tumor-propagating Cells

Due to the crucial role of miR-199b-5p in CD15+ and CD133+ cell expression, we investigated the regulation mechanisms of miR-199b-5p in CD15+/CD133+ MB cells. We isolated these cells from D341, D425, and Daoy MB cells using cell sorting analyses. The cells isolated were positive for both of the markers (Supplementary material, Fig. S4B). We then analyzed the expression of miR-199b-5p and Hes1 in these CD15+/CD133+ and CD15−/CD133− cells by RT-PCR analysis. The expression of miR-199b-5p was almost abolished in the CD15+/CD133+ cells, with opposite trends of expression between miR-199b-5p and its target Hes1 (Fig. 4A). Furthermore, Hes1 was upregulated in these CD15+/CD133+ cells. In Daoy cells, we also confirmed at the protein level that there was downregulation of Hes1 in CD15−/CD133− cells by Western blotting (Fig. 4B).

We then analyzed the methylation status of the CpG island upstream of the miR-199b-5p promoter in these selected CD15+/CD133+ cells, and remarkably, the methylation status of this CpG island was similar between the CD15+/CD133+ and CD15−/CD133− cells in these 3 MB cell lines (Fig. 4C).

Overall, these data show that in the MB tumor-propagating cells (CD15+/CD133+) the expression of miR-199b-5p is regulated mainly by a negative feedback loop driven by its target gene *Hes1* and that it is not regulated by the methylation status of the CpG island upstream of the miR-199b-5p promoter region.

A Network of Proteins Is Targeted by miR-199b-5p in Medulloblastoma

To determine which other pathways are regulated by miR-199b-5p, we used RPPAs to analyze the controlling network of interaction proteins of miR-199b-5p in MB cells, with a view to its future therapeutic application.

The expression and phosphorylation of the major proteins that might be deregulated in cancer progression were analyzed in the 199bSC1 miR-199b-5p stable clone and were compared with the empty vector clone and nontreated cells. Expression of those proteins that

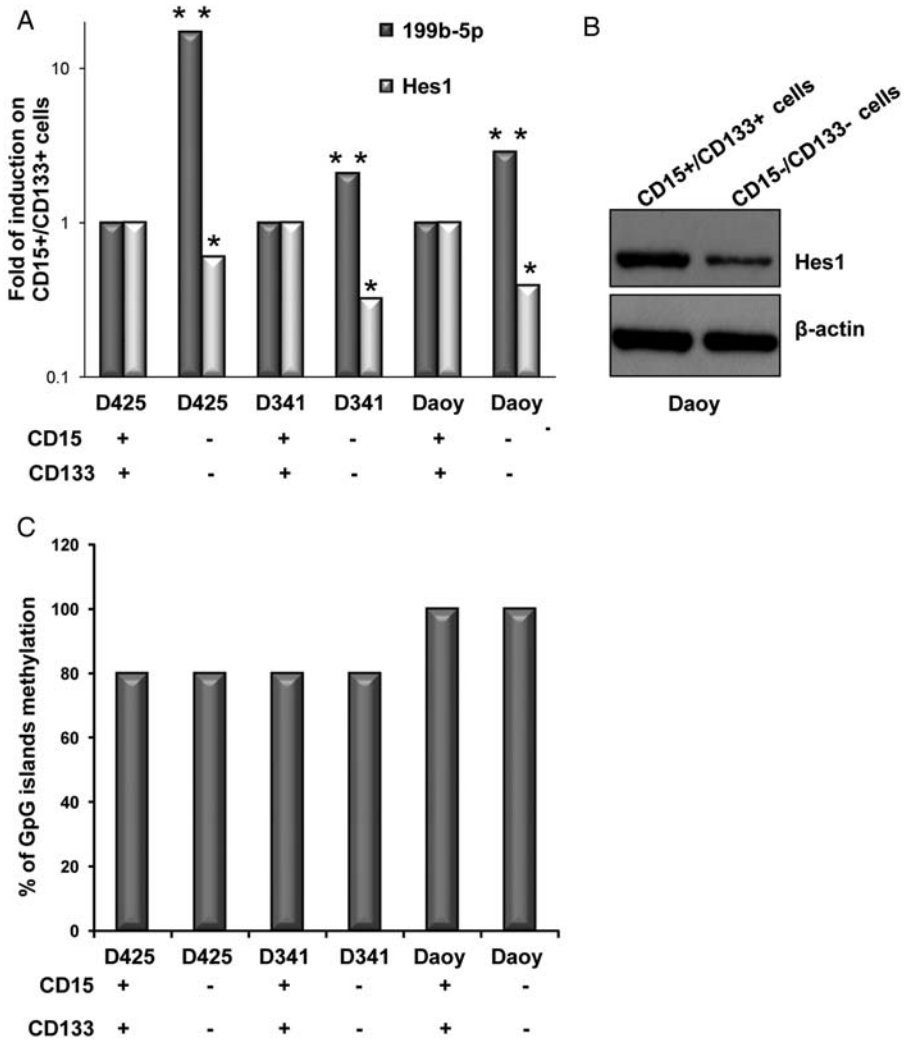

Fig. 4. Expression of miR-199b-5p and its target Hes1 in CD15+/CD133+ and CD15−/CD133− cells. (A) Relative expression of miR-199b-5p and Hes1 (as indicated) in CD15+/CD133+ cells sorted by fluorescence-activated cell sorting (FACS) from D425, D341, and Daoy cells, with their relative control CD15−/CD133− cells sorted from the same cells. Data are representative of 3 independent experiments. From left: $*P = .04$; .023, .037; $**P = .001$, .03, .001. (B) Representative Western blotting showing Hes1 expression in CD15+/CD133+ and CD15−/CD133− cells sorted from the Daoy cell line (as indicated). β-Actin expression shown for normalization. (C) Relative percentages of methylated CG dinucleotides in CpG islands upstream of the miR-199b-5p promoter, using bisulfite sequencing in CD15+/CD133+ cells extracted by FACS analysis from D425, D341, and Daoy cells, with their relative control of CD15−/CD133− cells extracted from the same cells. Data are means ± standard errors of 3 independent experiments.

were significantly deregulated is shown in the Supplementary material, Fig. S5A. Here, the phosphorylation of most of these proteins was downregulated in the miR-199b-5p clone in comparison with the empty vector (AKT S473, CHK1 S345, CHK2 S33-35, CYCL A, ERK 1-2T202-204, HSP70, KIP 1 P27, and MARCKS [myristoylated alanine-rich protein kinase C substrate]) S152-156, while that for EGFR Y992 and GRB2 was increased in the miR-199b-5p clone. The RPPA data were further confirmed by Western blotting in Daoy cells (Fig. 5A, left). The downregulation of Akt and ERK signaling by miR-199b-5p overexpression (using an adenovirus carrying miR-199b-5p) was also assayed in UW228 and ONS 76 cells and in another primary MB cell line (P.MB2) (Fig. 5A, right).

Our data augment the crucial role of miR-199b-5p in the impairment of signal transduction through the Akt and ERK pathways that maintain tumor-propagating cells and influence metastatic processes.

MiR-199b-5p Impairs Migration of Medulloblastoma Cells

Due to miR-199b-5p regulation of the Akt and ERK signaling pathways and its downregulation in metastatic-stage (M+) MB patients,[22] we speculated on its potential regulation of cellular proliferation, anchorage-independent growth, and cell migration in vitro. We thus confirmed the impairment of MB cell

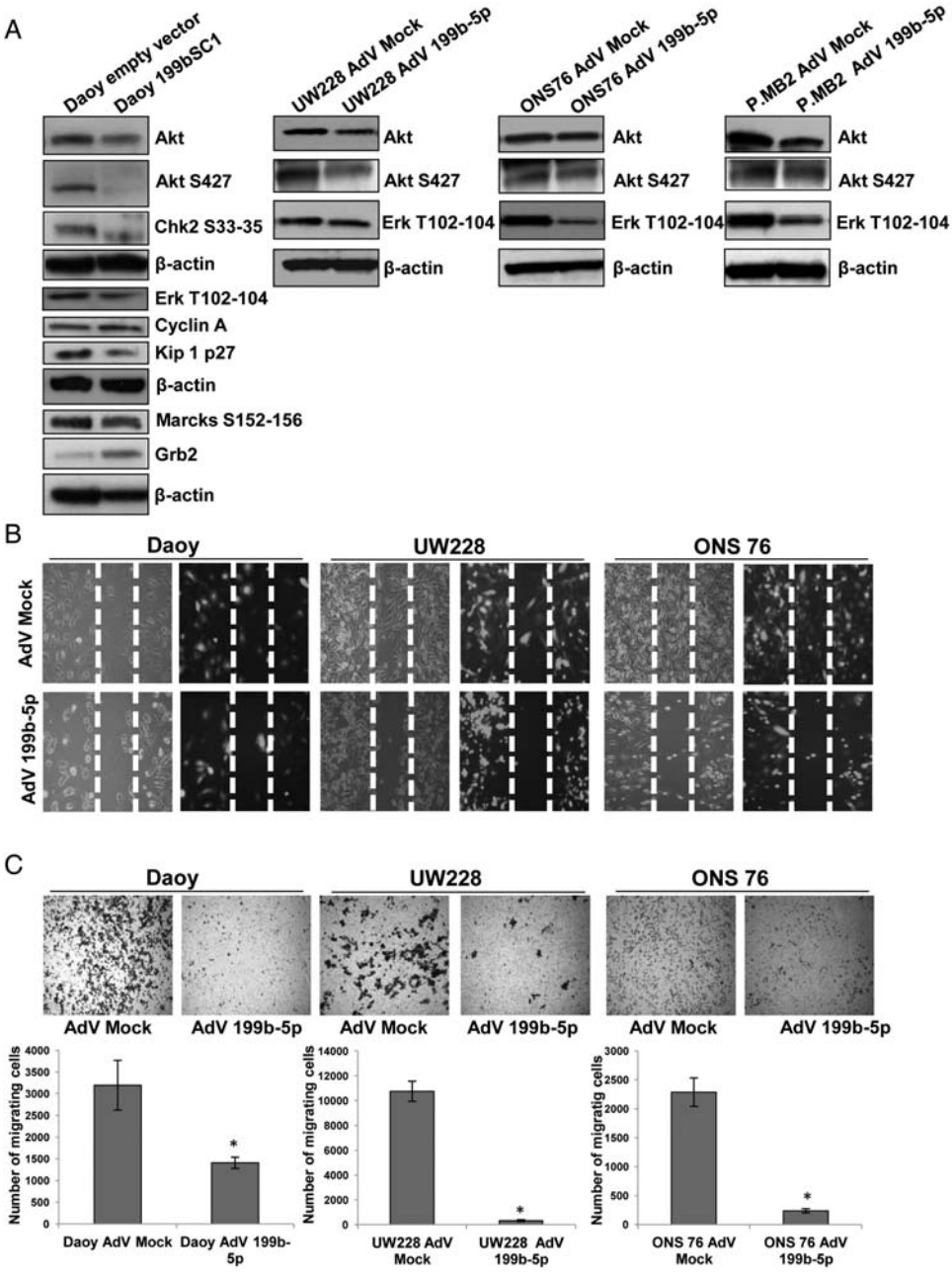

Fig. 5. Network of proteins targeted by miR-199b-5p in medulloblastoma. (A) Representative Western blotting of proteins (as indicated) regulated in the Daoy stable clone overexpressing miR-199b-5p (vs. Daoy empty-vector clone), and ONS 76, UW228, and primary MB cells (P.MB2) infected with an adenovirus carrying miR-199b-5p (vs. respective mock controls). β-Actin expression is shown for loading normalization. (B) Representative images of monolayer wound healing of Daoy, UW228, and ONS 76 MB cells treated with an adenovirus carrying miR-199b-5p (vs. mock control) after 24 h. Green fluorescent protein expression by the relevant adenovirus is shown for infection efficiency. Magnification, 100×. (C) Representative images of Daoy, UW228, and ONS 76 MB cells treated as in (B), for migration through a porous membrane toward fetal bovine serum-containing medium (upper panels), with relevant quantification (lower panels). Magnification, 100×. *$P = .01$, $P = .009$, $P = .02$ for the Daoy, UW28, and ONS 76 cells, respectively. Data are means ± standard errors of 3 independent experiments.

proliferation after overexpression of miR-199b-5p by adenovirus infection in both UW228 and ONS 76 cells (Supplementary material, Fig. S5B). In our previously published study,[22] we demonstrated that anchorage-independent growth can be affected by miR-199b-5p in Daoy cells. In the present study we further confirmed these data in ONS 76 cells infected with an adenovirus carrying miR-199b-5p (AdV 199b-5p), which showed a 50% reduction in colony formation in comparison with cells infected with the empty adenovirus (AdV Mock) (Supplementary material, Fig. S5C). The migration potential was then assayed by wound-healing and

two-dimensional migration experiments in Daoy, UW228, and ONS 76 cells upon miR-199b-5p overexpression, thus demonstrating overall a substantial reduction in the migratory properties of the cells (see Fig. 5B and C). Altogether, these data underline the inhibition of the metastatic behavior of MB cell lines in vitro upon miR-199b-5p overexpression.

Discussion

Although the study of the molecular pathogenesis of MB has advanced over the last 2 decades, prognostic evaluation continues to be based solely on clinical parameters.[48] Many studies conducted in recent years have supported the concept that the prognostic assessment of MB should routinely include investigations into molecular biomarkers.[49–53] Such supplementing of conventional diagnostics with molecular information should help to identify patients with aggressive tumors, who can then be treated with the most aggressive, and thus usually the most harmful, therapies. Novel therapies will result from a greater understanding of the disease process, and this is likely to involve small molecules that are designed to target specific pathways that become deregulated during MB oncogenesis.[48] In particular, new drugs that can inhibit the Notch pathway are being introduced into clinical trials, underlining the importance of this signaling in MB tumorigenesis.[11]

Identification of miRNAs with crucial roles in the regulation of tumor progression has opened new fields of studies in the search for new molecular markers for early diagnosis and prognosis of MB and for the development of new therapies. We previously defined the oncosuppressor function of miR-199b-5p in MB, with its targeting regulation of Hes1, a repressor transcriptional factor involved in the interplay between the signaling of the Notch and SHH pathways.[9,10] Indeed, Hes1 is also regulated by the SHH pathway, through a mechanism that does not involve γ-secretase-mediated Notch cleavage and that probably involves transcription factors other than recombination signal-binding protein Jκ in MB.[9] Moreover, a first demonstration of the independence of Hes1 from the Notch pathway was recently found in Ewing's sarcoma, indicating that Hes1 is uncoupled from Notch pathway activation.[54] Altogether, the data in the literature underline the importance of the inhibition of Hes1 for future therapy strategies in MB.

In the present study, we investigated the mechanism of this miR-199b-5p regulation and its other potential targets as a basis for the use of these findings for future clinical therapies.

We identified the miR-199b-5p autonomous promoter region and demonstrated that through a negative feedback loop, Hes1 binds to the miR-199b-5p promoter and inhibits its expression. Although miRNA biology has greatly advanced in the last few years, much of the effort to date has been focused on describing the targets of miRNAs rather than on understanding the regulation of the miRNA genes themselves. The nature of miRNA promoter/regulator elements remains one of the most interesting aspects for study in the near future.

In this paper, we identified the regulatory circuit that involves miR-199b-5p and its target Hes1. We showed that the downregulation of miR-199b-5p expression is influenced by methylation of a CpG island, a regulatory element that is upstream of its promoter region. Recent studies have shown that miRNAs located within CpG islands can be transcriptionally regulated by DNA methylation status and that patterns of methylation can vary in normal and cancer cells.[38,55] For example, miR-124a is hypermethylated in a cancer-specific manner, whereas miR-127 is methylated in both normal tissues and tumors,[15,16,56,57] and miR let-7a-3 is methylated in normal tissues and hypomethylated in some lung adenocarcinomas.[39,58] In our MB DNA tissues, the methylation of this miR-199b-5p CpG island is significantly increased compared with the internal control and with DNA from the peripheral blood of the same patients and is significantly inversely correlated with miR-199b-5p expression in MB tissues. These data demonstrate that methylation of the miR-199b-5p promoter is tumor specific and corresponds to a specific event that occurs during the development of MB tumors. Additionally, the 2 mechanisms of regulation—Hes1 negative feedback regulation on the miR-199b-5p promoter and its methylation status—cooperatively act to downregulate miR expression in MB, as demonstrated by miR-199b-5p upregulation once MB cells are treated with both a Hes1 inhibitor (DAPT) and a demethylation agent (AZA). Other genes localized in the same genomic region can be regulated by the same CpG island, which is here correlated to miR-199b-5p expression; this remains a particular issue for future studies to find other genes that are epigenetically regulated in MB.

It is well-known that each miRNA can regulate multiple targets, and thus in this paper we also investigated other potential targets of miR-199b-5p that might be involved in cancer stem-cell maintenance. Of interest, we found that *CD15* is an additional direct target of miR-199b-5p. CD15 is a carbohydrate antigen that has been reported to be a marker for tumor-propagating cells in the $Ptc^{+/-}$ MB mouse model; and in a subset of human MBs, it has been shown to be a predictor of patient survival.[41,42] We also confirmed the impairment of CD15 and CD133 expression in 2 primary human MB cell cultures. Future studies will address the potential for using the expression of these positive markers (CD15 and CD133) in tumors, together with miR-199b-5p, for diagnosis purposes for the stratification of MB risk. Thus, these analyses will be of importance and, we would expect, of great interest, especially with the crucial role of miR-199b-5p in controlling both of these targets (Hes1 and CD15), as these markers are expressed mainly in MB tumor-propagating cells. These data further support our previous findings, which showed impairment of tumor engraftment in an orthotopic mouse model of MB cells overexpressing miR-199b-5p in comparison with control MB cells

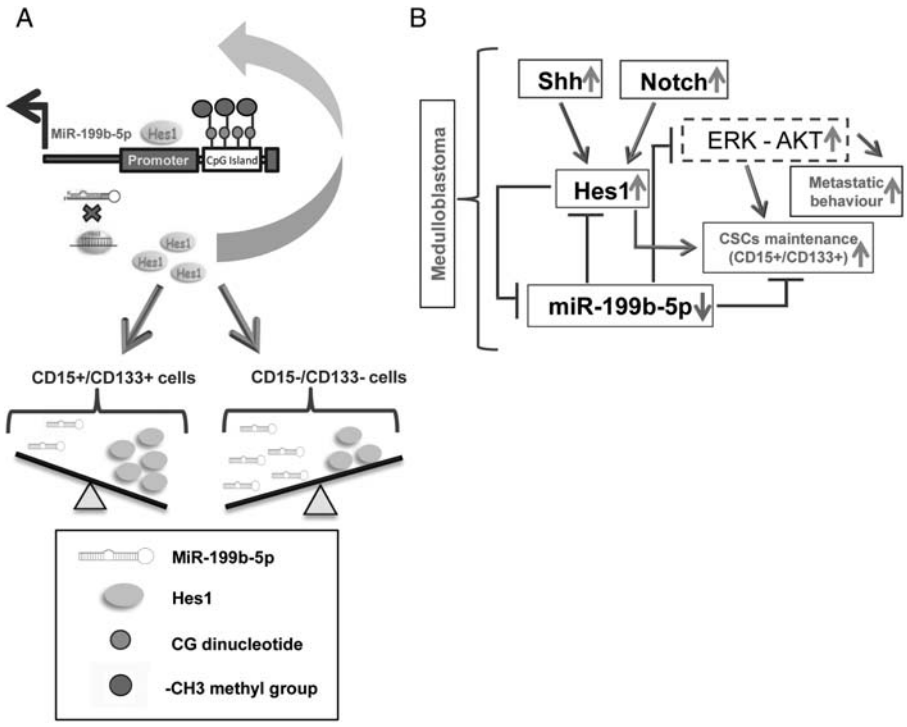

Fig. 6. Schematic models of the miR-199b-5p regulation mechanism and its interaction network in MB. (A) MiR-199b-5p expression is downregulated in MB by Hes1 (miR-199b-5p target, repressor transcriptional factor) binding to its promoter region, with negative feedback regulation, and by methylation of the CpG island upstream of its promoter region. In MB cancer stem cells identified by the CD15+/CD133+ markers, the expression of miR-199b-5p is downregulated by Hes1 overexpression. With CD15−/CD133− cells, miR-199b-5p is overexpressed compared with the positive counterpart, and Hes1 is downregulated. The methylation status of the CpG island is the same in the CD15+/CD133+ and CD15−/CD133− cells. (B) In MB, activation of SHH and Notch pathways directly upregulates Hes1, a dual effector of both of these signals. Conversely, Hes1 inhibits miR-199b-5p expression by binding to its promoter. Thus, miR-199b-5p cannot then regulate the ERK and Akt pathways, both of which are involved in metastasis processes and cancer stem cell (CSC) maintenance. Furthermore, miR-199b-5p cannot then target CD15, a marker of cancer stem cells in MB. The output of this finely tuned regulation is the maintenance of cancer stem-cell status and progression of MB to a metastatic stage.

both with stable cell clones and with adenovirus-infected cells.[20] Thus we can now speculate that the impairment of MB progression in vivo is also due to inhibition of the CD15 target. In the present study, we further found that Hes1 is upregulated in CD15+/CD133+ cells, while miR-199b-5p is downregulated, confirming the interplay between miR-199b-5p and its target also in these particular cancer stem-cell types in MB. These data are consistent with the microarray analysis of Read et al.,[41] who showed that CD15+ cells do have a distinct gene expression profile, characterized mostly by increased expression of genes associated with proliferation and self-renewal and decreased expression of genes involved in apoptosis and differentiation. Indeed CD15+ cells are more proliferative than CD15− cells, both in vitro and in vivo.[40] Moreover, the methylation status of the CpG island upstream of miR-199b-5p is similar between these CD15+/CD133+ cells and CD15−/CD133− cells, thus indicating further that in cancer stem cells, Hes1 is the major regulator of miR-199b-5p expression. Finally we confirmed a Hes1–miR-199b-5p loop of regulation involved in the maintenance of cancer stem-cell status, which is not controlled by an epigenetic mechanism of regulation for the control of the promoter region of miR-199b-5p. Although, this might be most likely to occur in vivo, the data presented here do not fully exclude other mechanisms of regulation that have yet to be investigated relating to MB.

Furthermore, again, it is known that each miRNA can control multiple target genes, and thus we studied other possible proteins as direct or indirect targets of miR-199b-5p, with the aim of applying this knowledge to future therapeutic approaches. For this, we used a protein array approach for the identification of a set of specific proteins that are involved in a variety of pathways deregulated in cancers. We showed that the levels of Akt phosphorylation on S473 and ERK 1-2 phosphorylation on T202-204 are decreased in the 199bSC1 Daoy clone, in comparison with the empty vector clone, and also in ONS 76, UW228, and primary MB cells. Akt represents a central mediator involved in the signal transduction of different growth-controlling pathways that involve phosphatidylinositol 3-kinases (PI3Ks), and activation of the PI3K/Akt pathway constitutes an important step in the molecular pathogenesis of MB.[59,60] Ras-ERK pathways are significantly upregulated in metastatic MB by activation of platelet-derived

growth factor.[61,62] For this reason, inhibition of the Akt and ERK pathways upon miR-199b-5p expression represents another promising therapeutic approach (see also additional discussion of the other proteins in the Supplementary section).

In conclusion, these data identify the involvement of miR-199b-5p in a regulatory circuit that is relevant to MB. We thus propose a schematic model of miR-199b-5p regulation during MB progression (Fig. 6A). Here, miR-199b-5p is downregulated by Hes1 binding to its promoter region through a negative feedback regulatory loop and by methylation of the CpG island upstream of its promoter region. MiR-199b-5p regulates expression of *CD15* and *CD133*, the 2 known markers of cancer stem cells in MB. Furthermore, to clarify the regulatory circuit of miR-199b-5p, we propose a model that defines the importance of miR-199b-5p in MB because of its regulation of the 2 main pathways, SHH and Notch, through its direct target Hes1, a dual effector of both of these signaling pathways. In MB, the upregulation of Hes1 in turn inhibits miR-199b-5p expression by binding to its promoter, according to which miR-199b-5p cannot regulate the ERK and Akt pathways, both of which are involved in metastasis processes and cancer stem-cell maintenance, and cannot target CD15, a substantial marker of cancer stem cells in MB. The output is the maintenance of cancer stem-cell behavior and substantial progression of MB to a metastatic stage.

Other reports currently show that in other tissue environments there are 2 additional targets of miRNA 199b-5p: the nuclear kinase Dyrk1a in heart and HIF1α in hepatocellular carcinoma.[63,64] The target HIF1α that was investigated in a recent study appears to also be of importance in MB tumorigenesis, as this tumor is highly affected by hypoxia status. Future studies will address these findings for their consequences in tumor therapy.

Moreover, the issues for our future studies will be to develop new carriers—for example, stable nucleic-acid lipid particles to deliver miR-199b-5p into the cerebellum of MB mouse models—to provide "proof of concept" studies for preclinical therapeutic applications.

Supplementary Material

Supplementary material is available at *Neuro-Oncology Journal* online (http://neuro-oncology.oxfordjournals.org/).

Acknowledgments

The authors would like to thank the CEINGE Service Facility platforms for supporting the projects with their extensive state-of-the-art methodologies and their automated setups including the Sequencing Core and the FACS Core Laboratory, headed by Prof. Luigi Del Vecchio; Dr. Maurizio Franco Mariani Group Head of R&D; Advanced Accelerator Applications (AAA) for providing helpful discussions for future therapeutic applications of miR-199-5p in brain cancer; and the NICHD Brain and Tissue Bank, University of Maryland, Department of Pediatrics (Baltimore, Maryland, USA) for sharing healthy control cerebellum tissue.

Conflict of interest statement. None declared.

Funding

This study was financed by FP7-Tumic HEALTH-F2-2008-201662 (to MZ) and Fondazione Neuroblastoma Italiana "Progetto Pensiero"(MZ), and Associazione Italiana per la Ricerca sul Cancro AIRC, 2009–2011 (to MZ).

References

1. Ellison D. Classifying the medulloblastoma: insights from morphology and molecular genetics. *Neuropathol Appl Neurobiol*. 2002;28(4):257–282.
2. Gajjar A, Hernan R, Kocak M, et al. Clinical, histopathologic, and molecular markers of prognosis: toward a new disease risk stratification system for medulloblastoma. *J Clin Oncol*. 2004;22(6):984–993.
3. Ellison DW, Clifford SC, Gajjar A, Gilbertson RJ. What's new in neuro-oncology? Recent advances in medulloblastoma. *Eur J Paediatr Neurol*. 2003;7(2):53–66.
4. Gilbertson RJ, Ellison DW. The origins of medulloblastoma subtypes. *Annu Rev Pathol*. 2008;3:341–365.
5. Huse JT, Holland EC. Targeting brain cancer: advances in the molecular pathology of malignant glioma and medulloblastoma. *Nat Rev Cancer*. 2010;10(5):319–331.
6. Eberhart CG. In search of the medulloblast: neural stem cells and embryonal brain tumors. *Neurosurg Clin N Am*. 2007;18(1):59–69, viii–ix.
7. Jenkins D. Hedgehog signalling: emerging evidence for non-canonical pathways. *Cellular Signalling*. 2009;21(7):1023–1034.
8. Lauth M, Toftgard R. Non-canonical activation of GLI transcription factors: implications for targeted anti-cancer therapy. *Cell Cycle (Georgetown, Tex.)*. 2007;6(20):2458–2463.
9. Morton JP, Lewis BC. Shh signaling and pancreatic cancer: implications for therapy? *Cell Cycle (Georgetown, Tex.)*. 2007;6(13):1553–1557.
10. Fan X, Mikolaenko I, Elhassan I, et al. Notch1 and notch2 have opposite effects on embryonal brain tumor growth. *Cancer Res*. 2004;64(21):7787–7793.
11. Hallahan AR, Pritchard JI, Hansen S, et al. The SmoA1 mouse model reveals that notch signaling is critical for the growth and survival of sonic hedgehog-induced medulloblastomas. *Cancer Res*. 2004;64(21):7794–7800.
12. Ingram WJ, McCue KI, Tran TH, Hallahan AR, Wainwright BJ. Sonic Hedgehog regulates Hes1 through a novel mechanism that is independent of canonical Notch pathway signalling. *Oncogene*. 2008;27(10):1489–1500.

13. Schreck KC, Taylor P, Marchionni L, et al. The Notch target Hes1 directly modulates Gli1 expression and Hedgehog signaling: a potential mechanism of therapeutic resistance. *Clin Cancer Res*. 2010;16(24):6060–6070.
14. Fouladi M, Stewart CF, Olson J, et al. Phase I trial of MK-0752 in children with refractory CNS malignancies: a pediatric brain tumor consortium study. *J Clin Oncol*. 2011;29(26):3529–3534.
15. Fan X, Matsui W, Khaki L, et al. Notch pathway inhibition depletes stem-like cells and blocks engraftment in embryonal brain tumors. *Cancer Res*. 2006;66(15):7445–7452.
16. Hatton BA, Villavicencio EH, Pritchard J, et al. Notch signaling is not essential in sonic hedgehog-activated medulloblastoma. *Oncogene*. 2010;29(26):3865–3872.
17. Julian E, Dave RK, Robson JP, Hallahan AR, Wainwright BJ. Canonical Notch signaling is not required for the growth of Hedgehog pathway-induced medulloblastoma. *Oncogene*. 2010;29(24):3465–3476.
18. Ferretti E, De Smaele E, Miele E, et al. Concerted microRNA control of Hedgehog signalling in cerebellar neuronal progenitor and tumour cells. *EMBO J*. 2008;27(19):2616–2627.
19. Ferretti E, De Smaele E, Po A, et al. MicroRNA profiling in human medulloblastoma. *Int J Cancer*. 2009;124(3):568–577.
20. Lu Y, Ryan SL, Elliott DJ, et al. Amplification and overexpression of Hsa-miR-30b, Hsa-miR-30d and KHDRBS3 at 8q24.22-q24.23 in medulloblastoma. *PLoS One*. 2009;4(7):e6159.
21. Northcott PA, Fernandez LA, Hagan JP, et al. The miR-17/92 polycistron is up-regulated in sonic hedgehog-driven medulloblastomas and induced by N-myc in sonic hedgehog-treated cerebellar neural precursors. *Cancer Res*. 2009;69(8):3249–3255.
22. Pierson J, Hostager B, Fan R, Vibhakar R. Regulation of cyclin dependent kinase 6 by microRNA 124 in medulloblastoma. *J Neurooncol*. 2008;90(1):1–7.
23. Turner JD, Williamson R, Almefty KK, et al. The many roles of microRNAs in brain tumor biology. *Neurosurg Focus*. 2010;28(1):E3.
24. Uziel T, Karginov FV, Xie S, et al. The miR-17∼92 cluster collaborates with the Sonic Hedgehog pathway in medulloblastoma. *Proc Natl Acad Sci USA*. 2009;106(8):2812–2817.
25. Garzia L, Andolfo I, Cusanelli E, et al. MicroRNA-199b-5p impairs cancer stem cells through negative regulation of HES1 in medulloblastoma. *PLoS One*. 2009;4(3):e4998.
26. Fruhwald MC, O'Dorisio MS, Dai Z, et al. Aberrant promoter methylation of previously unidentified target genes is a common abnormality in medulloblastomas–implications for tumor biology and potential clinical utility. *Oncogene*. 2001;20(36):5033–5042.
27. Lindsey JC, Anderton JA, Lusher ME, Clifford SC. Epigenetic events in medulloblastoma development. *Neurosurg Focus*. 2005;19(5):E10.
28. Northcott PA, Nakahara Y, Wu X, et al. Multiple recurrent genetic events converge on control of histone lysine methylation in medulloblastoma. *Nat Genet*. 2009;41(4):465–472.
29. Irizarry RA, Ladd-Acosta C, Wen B, et al. The human colon cancer methylome shows similar hypo- and hypermethylation at conserved tissue-specific CpG island shores. *Nat Genet*. 2009;41(2):178–186.
30. Croce CM. Causes and consequences of microRNA dysregulation in cancer. *Nat Rev Genet*. 2009;10(10):704–714.
31. Davalos V, Esteller M. MicroRNAs and cancer epigenetics: a macrorevolution. *Curr Opin Oncol*. 2010;22(1):35–45.
32. Garzon R, Calin GA, Croce CM. MicroRNAs in Cancer. *Annu Rev Med*. 2009;60:167–179.
33. Ryan BM, Robles AI, Harris CC. Genetic variation in microRNA networks: the implications for cancer research. *Nat Rev Cancer*. 2010;10(6):389–402.
34. Waldman SA, Terzic A. A study of microRNAs in silico and in vivo: diagnostic and therapeutic applications in cancer. *FEBS J*. 2009;276(8):2157–2164.
35. Tsang J, Zhu J, van Oudenaarden A. MicroRNA-mediated feedback and feedforward loops are recurrent network motifs in mammals. *Mol Cell*. 2007;26(5):753–767.
36. Livak KJ, Schmittgen TD. Analysis of relative gene expression data using real-time quantitative PCR and the 2(-Delta Delta C(T)) Method. *Methods*. 2001;25(4):402–408.
37. Panchision DM, Chen HL, Pistollato F, Papini D, Ni HT, Hawley TS. Optimized flow cytometric analysis of central nervous system tissue reveals novel functional relationships among cells expressing CD133, CD15, and CD24. *Stem Cells*. 2007;25(6):1560–1570.
38. Toyota M, Suzuki H, Sasaki Y, et al. Epigenetic silencing of microRNA-34b/c and B-cell translocation gene 4 is associated with CpG island methylation in colorectal cancer. *Cancer Res*. 2008;68(11):4123–4132.
39. Petricoin EF, 3rd, Bichsel VE, Calvert VS, et al. Mapping molecular networks using proteomics: a vision for patient-tailored combination therapy. *J Clin Oncol*. 2005;23(15):3614–3621.
40. Petricoin EF, 3rd, Espina V, Araujo RP, et al. Phosphoprotein pathway mapping: Akt/mammalian target of rapamycin activation is negatively associated with childhood rhabdomyosarcoma survival. *Cancer Res*. 2007;67(7):3431–3440.
41. Wulfkuhle JD, Aquino JA, Calvert VS, et al. Signal pathway profiling of ovarian cancer from human tissue specimens using reverse-phase protein microarrays. *Proteomics*. 2003;3(11):2085–2090.
42. Espina V, Mehta AI, Winters ME, et al. Protein microarrays: molecular profiling technologies for clinical specimens. *Proteomics*. 2003;3(11):2091–2100.
43. Clayton EL, Sue N, Smillie KJ, et al. Dynamin I phosphorylation by GSK3 controls activity-dependent bulk endocytosis of synaptic vesicles. *Nature Neuroscience*. 2010;13(7):845–851.
44. Abderrahmani A, Niederhauser G, Lenain V, Regazzi R, Waeber G. The hairy and enhancer of split 1 is a negative regulator of the repressor element silencer transcription factor. *FEBS Lett*. 2005;579(27):6199–6204.
45. Ward RJ, Lee L, Graham K, et al. Multipotent CD15+ cancer stem cells in patched-1-deficient mouse medulloblastoma. *Cancer Res*. 2009;69(11):4682–4690.
46. Read TA, Fogarty MP, Markant SL, et al. Identification of CD15 as a marker for tumor-propagating cells in a mouse model of medulloblastoma. *Cancer Cell*. 2009;15(2):135–147.
47. Kertesz M, Iovino N, Unnerstall U, Gaul U, Segal E. The role of site accessibility in microRNA target recognition. *Nat Genet*. 2007;39(10):1278–1284.
48. Pfister S, Remke M, Benner A, et al. Outcome prediction in pediatric medulloblastoma based on DNA copy-number aberrations of chromosomes 6q and 17q and the MYC and MYCN loci. *J Clin Oncol*. 2009;27(10):1627–1636.
49. Gilbertson R, Wickramasinghe C, Hernan R, et al. Clinical and molecular stratification of disease risk in medulloblastoma. *Br J Cancer*. 2001;85(5):705–712.
50. Polkinghorn WR, Tarbell NJ. Medulloblastoma: tumorigenesis, current clinical paradigm, and efforts to improve risk stratification. *Nat Clin Pract Oncol*. 2007;4(5):295–304.

51. Fernandez-Teijeiro A, Betensky RA, Sturla LM, Kim JY, Tamayo P, Pomeroy SL. Combining gene expression profiles and clinical parameters for risk stratification in medulloblastomas. *J Clin Oncol*. 2004;22(6):994–998.
52. Eberhart CG, Kratz J, Wang Y, et al. Histopathological and molecular prognostic markers in medulloblastoma: c-myc, N-myc, TrkC, and anaplasia. *J Neuropathol Exp Neurol*. 2004;63(5):441–449.
53. Rutkowski S, von Bueren A, von Hoff K, et al. Prognostic relevance of clinical and biological risk factors in childhood medulloblastoma: results of patients treated in the prospective multicenter trial HIT'91. *Clin Cancer Res*. 2007;13(9):2651–2657.
54. Bennani-Baiti IM, Aryee DN, Ban J, et al. Notch signalling is off and is uncoupled from HES1 expression in Ewing's sarcoma. *J Pathol*. 2011;225(3):353–363.
55. Lujambio A, Esteller M. CpG island hypermethylation of tumor suppressor microRNAs in human cancer. *Cell Cycle*. 2007;6(12):1455–1459.
56. Saito Y, Liang G, Egger G, et al. Specific activation of microRNA-127 with downregulation of the proto-oncogene BCL6 by chromatin-modifying drugs in human cancer cells. *Cancer Cell*. 2006;9(6):435–443.
57. Lujambio A, Ropero S, Ballestar E, et al. Genetic unmasking of an epigenetically silenced microRNA in human cancer cells. *Cancer Res*. 2007;67(4):1424–1429.
58. Brueckner B, Stresemann C, Kuner R, et al. The human let-7a-3 locus contains an epigenetically regulated microRNA gene with oncogenic function. *Cancer Res*. 2007;67(4):1419–1423.
59. Franke TF. PI3K/Akt: getting it right matters. *Oncogene*. 2008;27(50):6473–6488.
60. Hartmann W, Digon-Sontgerath B, Koch A, et al. Phosphatidylinositol 3′-kinase/AKT signaling is activated in medulloblastoma cell proliferation and is associated with reduced expression of PTEN. *Clin Cancer Res*. 2006;12(10):3019–3027.
61. Yuan L, Santi M, Rushing EJ, Cornelison R, MacDonald TJ. ERK activation of p21 activated kinase-1 (Pak1) is critical for medulloblastoma cell migration. *Clinical & Experimental Metastasis*. 2010;27(7):481–491.
62. Abouantoun TJ, MacDonald TJ. Imatinib blocks migration and invasion of medulloblastoma cells by concurrently inhibiting activation of platelet-derived growth factor receptor and transactivation of epidermal growth factor receptor. *Molecular Cancer Therapeutics*. 2009;8(5):1137–1147.
63. da Costa Martins PA, Salic K, Gladka MM, et al. MicroRNA-199b targets the nuclear kinase Dyrk1a in an auto-amplification loop promoting calcineurin/NFAT signalling. *Nature Cell Biology*. 2010;12(12):1220–1227.
64. Wang C, Song B, Song W, et al. Underexpressed microRNA-199b-5p targets Hypoxia-Inducible Factor-1alpha in hepatocellular carcinoma and predicts prognosis of hepatocellular carcinoma patients. *Journal of Gastroenterology and Hepatology*. 2011;26(11):1630–1637.